Dislocation Networks in Crystals*

Taira SUZUKI and Hideji SUZUKI

The Research Institute for Iron, Steel and Other Metals

(Received September 20, 1954)

Synopsis

The conditions to make dislocation networks exist with sufficient life time were examined. It was found that the hexagonal plane network formed parallel to {113} planes was relatively more stable than others, for instance {111} type in a face-centred cubic crystal. This prediction came only from a local maintenance of mechanical balance at a node. The space arrangements of those networks have certain intimate connection with their persistence in crystals. A reasonable estimation of the density of dislocations in annealed crystal from the present picture gave 2×10^6 cm/cm^3, which was fairly smaller than usually accepted values.

The motion of dislocation network of {113} type under externally applied small stress was studied, which gave an alternative explanation for the micro-creep. The order of magnitude of the micro-creep rate could be satisfactorily accounted for. A number of jogs formed along dislocation lines during the motion of networks account for the increase of critical shear stress of crystals after micro-creep. The orientation dependence of such a micro-creep hardening predicted theoretically showed a fair agreement with experiments.

I. Introduction

The hexagonal form of dislocation network was first predicted in the lecture made by Mott(1), following a suggestion by Frank. His prediction was very important and fruitful in nature. In fact, it was confirmed by the very recent success of Hedges and Mitchell(2) in making dislocation lines visible in a transparent silver-bromide crystal.

One of the essential subjects remained unsolved in the theory of dislocation is the problem concerned with the space distribution of dislocation networks and with certain physical origins to decide the size of their mesh. The theory is still in its infancy.

The first aim of the present research was to construct the basic geometry of dislocation network. The dislocations in a crystal are, of course, thermodynamically unstable. So we must discuss first the conditions making certain dislocation patterns remain with sufficiently long life time. Further, the mechanical properties seeming very sensitive to those patterns are reproducible, within certain limits, on a number of crystals which are made separately but are otherwise macroscopically the same, say, in respects of crystallographic orientation, purity, etc.. Although it may be more rational to say that our knowledges of delicate and systematic fluctuations in experimental results are wanting, this fact leads us to the conclusion that dislocation

* The 778th report of the Research Institute for Iron, Steel and Other Metals. The main part of this paper was read at International Conference of Theoretical Physics held at Kyoto on Sept. 1953.

(1) N. F. Mott, Proc. Phys. Soc., **B 64** (1951), 729.

(2) J. M. Hedges and J. W. Mitchell, Phil. Mag., **44** (1953), 223.

networks realizable must mechanically be balanced at least locally and also balanced in some way as a whole.

Some possible space arrangements of dislocation networks will be discussed and separate considerations must be made to decide how the formation of 'mosaic' block structure is connected with the mechanism of crystal growth. The space distribution thus obtained may be very interesting and will have many profound effects on the phenomena originating in crystal imperfections.

The motion of plane network of dislocations in the sense of that of small angle crystal boundary, on which the discussions were confined only to that of simple array of edge dislocations, was discussed more in rigour and more in concrete. This yielded an alternative mechanism for micro-creep and its related phenomena in a face-centred cubic crystal.

Since Frank and Read[3] proposed the theory of multiplication for crystalline slip, a number of works have been made with the aim to solve the mechanism of slip and work-hardening. The problem, however, is most still unsolved, as Mott called our attention to some difficulties involved[4].

Dislocation networks yield undoubtedly some Frank-Read sources. In this sense, it must be important to note that the most 'stable' networks have certain topologically peculiar characteristics as slip sources and those may throw a light upon such problems. The discussion of slip and work-hardening of face-centred cubic crystals from this point of view were reported elsewhere[5][6].

II. Basic geometry of dislocation network: Preliminary

1. Plane network

For several dislocation lines meeting at a point it is geometrically necessary that the sum of their Burgers vectors is zero. Only this topological condition found by Frank[7] permits any number of perfect dislocation lines to meet at a point and it gives a two-fold, three-fold, etc. node. So long as the dislocations are dissociated into partials in the sence of Heidenreich and Shockley[8], they will be constrained to lie in {111} planes in a face-centred cubic crystal (Burgers vector $\boldsymbol{b} = \frac{a}{2}\langle 110\rangle$), but no restriction is placed on their directions in those planes. Thus, three dislocations meeting at a node in otherwise prefect crystal subject to no externally applied stress could be straight owing to their line tension, would lie in one plane, and would make angles of 120° with one another, if their line tensions are equal to one another.

(3) F.C. Frank and W.T. Read, Phys. Rev., **79** (1950), 722.
(4) N.F. Mott, read at Int. Nat. Conf. Theoretical Physics held at Kyoto on Sept. 1953; to be published
(5) H. Suzuki and F.E. Fujita., J. Phys. Soc. Japan, **9** (1954), 428; H. Suzuki, J. Phys. Soc. Japan, **9** (1954), 531.
(6) T. Suzuki, Sci. Rep., RITU, **A 6** (1954), 309.
(7) F.C. Frank, Phil. Mag., **42** (1951), 809.
(8) R.D. Heidenreich and W. Shockley, *Report of a Conference on the Strength of Solids* (London: Phys. Soc., 1948), 57.

Three dislocations mechanically balanced at a node thus give a hexagonal network. When parallel elements forming a hexagonal network are of the same Burgers vectors, they will give a regular plane network[9].

2. Polyhedral network

As for a three-dimensional network of dislocations, there can be two cases. The first is that, in which the dislocations meeting at a node are never in a plane in a mechanically balanced state. Another will be discussed in the next. The three-dimensional networks composed of four-fold nodes is realized in a diamond lattice structure and in the form of orthic-tetrakaidecahedron(Fig. 1). A mechanical equilibrium, however, is maintained only in the former.

Four dislocations leaving from a node in a diamond structure of network are parallel to <111> directions respectively, and so this is an elementary network formed in a body-centred cubic crystal, in which Burgers vector $\boldsymbol{b}=\frac{a}{2}$ <111>. On the other hand, three-dimensional orthic-tetrakaidecahedron network may also exist in a certain case in a face-centred cubic crystal as discussed later.

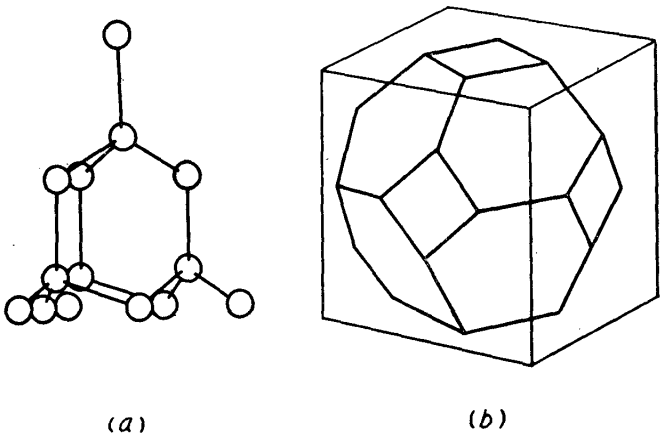

Fig. 1. Three-dimensional network.
(a) Similar to diamond lattice, possible in body-centred cubic lattice.
(b) Orthic-tetrakaidecahedron.

3. Space arrangement of plane networks

As already discussed, the most elementary network in a face-centred cubic crystal is the plane network of hexagonal form. The next important problem is to know the space arrangement of these plane networks in an annealed crystal. The condition of mechanical balance assumed at a node of dislocation network must be also maintained at a node in the boundary, where several plane networks meet. In other words, starting from nodes in the boundary under a mechanical balance we can obtain a certain space arrangement of plane networks, which may define the surfaces of a certain polyhedron. A crystalline body must be constructed out of a number of such a polyhedron with little gap.

Among the possible polyhedrons satisfying the last condition orthic-tetrakaidecahedron has the minimum surface. In this case hexagonal networks are formed in hexagonal surfaces and rectangular ones in cubic surfaces. A plane network in the surfaces of this polyhedron, however, can not be balanced mechanically at the edge of the polyhedron with the other two plane networks meeting at the edge[10].

(9) N. Thompson, Proc. Phys. Soc., **B 66** (1953), 481.
(10) C. S. Smith, Acta Metallurgica, **1**, (1953), 295.

It is also possible to fill up a crystal space with a more simple arrangement of hexagonal networks, of which boundaries can be formed by only triple junctions of dislocation; in other words, three plane networks meet at those boundaries. This type of the structure is illustrated by 'honeycomb' structure in Fig. 4.

III. Stable network of dislocations

1. Conditions of existence after anneal

In crystals either grown up from the melt or made after recrystallization, there must be some apparently stable configuration of dislocation networks, which can persist in a sufficiently long life after practical duration of anneal.

Dislocations in a crystal is, of course, thermodynamically unstable. They can not exist in otherwise perfect crystals by the minimum free energy condition, and so the configurations of the networks in annealed crystals must satisfy the following conditions. It is necessary to maintain a mechanically equilibrium configuration at least locally.

(a) Dislocations are dissociated into partials in the sense of Heidenreich and Shockley[8] and decrease their self-energies.

(b) A mechanical balance between line tensions at a node is satisfied and the line between neighbouring nodes is as short as possible.

Not to transform to another configuration by glide motion alone.

(c) Diffusion is always needed through sufficiently long path for a transformation to another stable configuration. This means that regular networks spread over a sufficient extent.

2. Plane network of dislocations in an annealed face-centred cubic crystal

The relative stability of plane networks conceivable in a face-centred cubic lattice can be described in the following way, which is applicable to any more general dislocation network. All the possible networks must be obtained from the basic network of a certain type considered.

The basic one for the plane network may conveniently be defined as composed of three screw dislocations. Any regular plane network can be obtained by rotating this by certain degrees around coordinate axes of orthogonal set appropriately fixed to the original basic network.

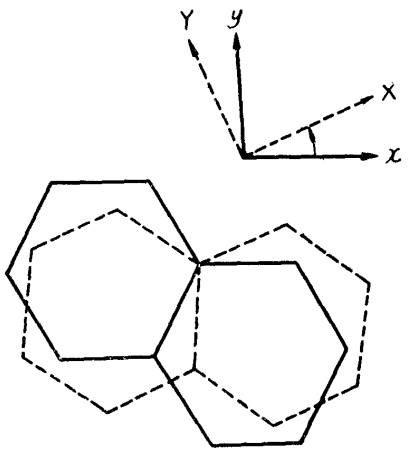

Fig. 2. Rotation of basic network around z-axis.

From Frank's condition for a triple junction, the three dislocations define necessarily a {111} plane, in which their vectors must lie; that is the vector plane. A mechanical balance assumed at a node yields the following two cases and no more. First, all three dislocations lie in the vector plane, and second, only one of them in that plane. Accordingly, it is sufficient to start from the latter case.

Let the coordinate system fix to the basic network plane (xy-plane) as shown in Fig. 2. Any possible plane network will be able to be obtained by a certain rotation around X-axis, which is fixed to one of the dislocation lines, following a rotation around Z-axis.

A rotation around X-axis including zero degree alone will give no stable configuration other than an equilibrium distribution of Eshelby-Frank-Nabarro[11] or of Leibfried[12] attained after some glide motion of dislocations induced by repulsive forces between them.

According to the above reason, it is sufficient to consider the dislocation in X-position lying in the vector plane. The two others are placed in the neighbouring {111} planes symmetrically situated to the vector plane respectively. Let the X-dislocation be of a pure screw type. A force to hold a mechanical balance will act so as to inforce or resist the rotation around X-axis. On the other hand, when it is of a pure edge type, the more the rotation increases, the more the deviation increases from the position symmetrical to the two others, as illustrated in Fig. 3. The rotation axis, thus, tends to move towards a new position, say X', so as a mechanical balance may be maintained.

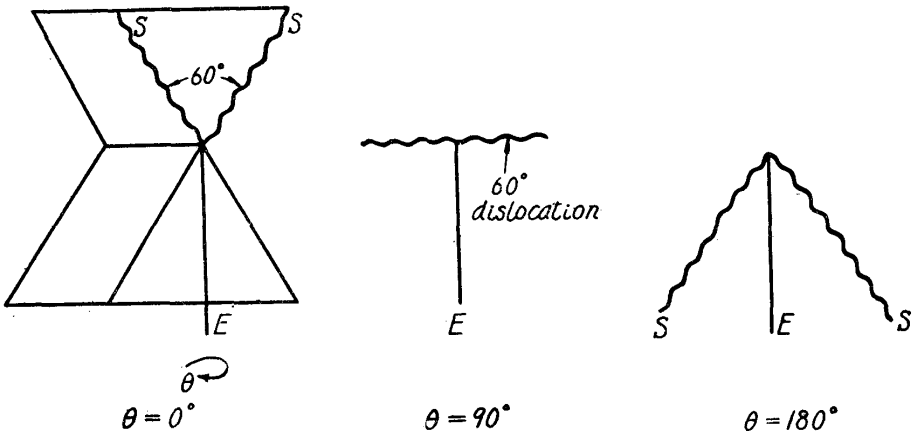

Fig. 3. Rotation around X-axis following that around z-axis, where X-axis is parallel to the dislocation line of pure edge type. θ means the rotation angle.

In other cases, X-dislocation being neither a pure screw nor a pure edge, some force will act the rotation axis and will move it in the direction parallel to the pure screw dislocation line or to a mixed one (X', 60°-dislocation).

As a result, so far as the glide motion and the creation of vacancies can easily occur, a certain force to get a mechanical balance inforces the network to occupy such positions as X-dislocation becomes a pure edge or screw type. Thus, we can find the plane of a hexagonal network relatively stable as follows:

When the dislocation in the vector plane is of a pure screw type, the two others are almost pure edge ones and, thus, the network lies in a {113} plane. Putting the line energies of screw and edge dislocations W_S and W_E respectively, the

(11) J. D. Eshelby, F. C. Frank and F. R. N. Nabarro, Phil. Mag., **42**, (1951), 351.
(12) G. Leibfried, Z. Phys., **130** (1951), 214.

mechanical balance between them will be attained, if the relation $W_S = 0.578\, W_E$ is correct. This relation almost satisfies the theoretical result, $W_S = (1-\nu)W_E$, where ν is Poisson's ratio.

When the dislocation considered is of a pure edge type, the rotation around X-axis should be zero at a mechanical balance. In this case, the two others are screw dislocations as illustrated in Fig. 3 and the network lies in a {111} plane parallel to the vector plane. Thus, we have obtained the two types of plane networks of dislocations, {113} and {111}, from the conditions (a) and (b) mentioned in the beginnning of this section.

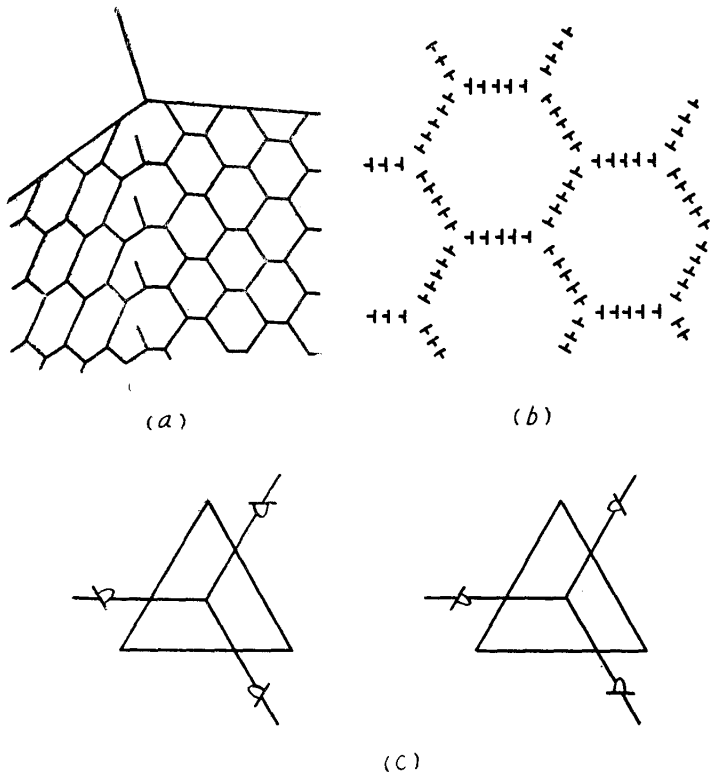

Fig. 4. (a) Honeycomb structure composed of regular plane networks.
(b) Plan view normal to the boundary line, which illustrates a simplified configuration in the vector plane by the substitution of simple edge dislocation wall.
(c) Two kinds of the regular boundary configuration at neighbouring positions along the boundary line.

The stress field of the screw dislocation is purely shear without dilatation. On this account, it fails to give the one origin of persistence to the dislocation network as discussed later in detail. Furthermore, the more the number of screw dislocations increases, the more they will diminish the resistance against the motion of dislocation nodes. For such reasons the elements in the dislocation network remaining in an annealed crystal would be more favourable to the edge dislocations than to the screw. The coarsening of {111} type network, in fact, does not need the vacancy diffusion, and so its life is necessarily shorter than that of {113} type.

3. Process of formation of dislocation network

(i) Size of hexagonal mesh

Now consider the case that a number of dislocations are introduced into crystal by plastic deformation or vacancy condensation[13][14]. In either case a prolonged annealing will give rise to a space distribution of dislocation networks at a very

(13) F. Seitz, Phys. Rev., **79** (1950), 890.
(14) F. E. Fujita, Sci. Rep. RITU, **A 6** (1954), 125.

early stage of annealing, and to certain changes in its configuration and in the size of hexagonal mesh. The hexagonal mesh has always a tendency to enlarge its size owing to repulsive forces between dislocations.

The coarsening of dislocation network composed of dislocations in different slip planes is necessarily accompanied by the climb of a part of those members. The process is, therefore, controlled by the frequency of climb of nodes or by the flux of vacancies.

If the coarsening rate of the network mesh is controlled only by the latter, it will be not unreasonable to assume that the released energy of annihilated dislocations is perfectly used for driving the diffusion. On the basis of this assumption we obtain

$$\frac{1}{l}\frac{\partial l}{\partial t}=\alpha\frac{D}{kT}\frac{\Omega l\mu}{L^4}\left(\ln\frac{l}{2r_0}-1\right) \qquad (1)$$

as the coarsening rate of network mesh in a crude approximation, where α is a constant with the magnitude of about 20cm, D the self-diffusion coefficient, Ω the volume occupied by a vacancy, l the mesh of the network, μ the rigidity modulus, L the average dimension of a regular region of a network, r_0 the cut-off radius of a dislocation to obtain the true strain energy. In the case of copper substituting reasonable values into (1) as $D=10^{-8}\,\mathrm{cm^{-2}\,sec^{-1}}$, $T=1300^{\circ}\mathrm{K}$, $\Omega=1.2\times10^{-23}\,\mathrm{cm^3}$, $l=10^{-4}\,\mathrm{cm}$, $\mu=4\times10^{11}$ dyne $\mathrm{cm^{-2}}$, $L\simeq10^{-3}\sim10^{-2}\,\mathrm{cm}$, $r_0=5\times10^{-8}\mathrm{cm}$, we have

$$\frac{1}{l}\frac{\partial l}{\partial t}\simeq10^{-4}\sim1\ \mathrm{sec^{-1}}$$

Therefore, even in the slowest case the mesh size increases about a half during the annealing by an hour. This magnitude of the rate is of course too large in comparison with usual experiences.

We shall next evaluate the rate controlled by the frequecy of climb of nodes. To complete the climb of the node A in Fig. 5 a jog formed at A should travel to B or a jog with the opposite sign should travel from B to A, because the energy of the jog is usually greater than the work done by the climb of the node. The travel of a jog also should be accompanied by the generation or

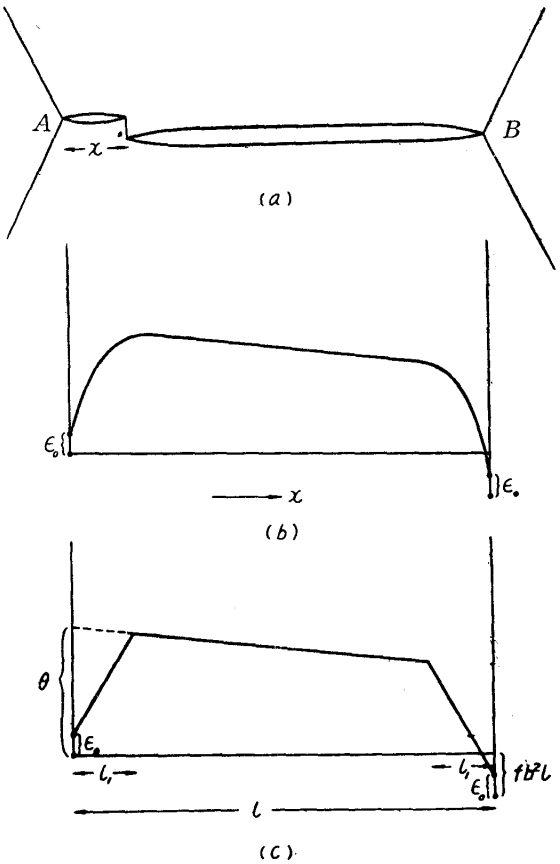

Fig. 5. Activation energy for the climb of a node.
(a) Migration of a jog required for the climb of the node.
(b) Potential energy of the jog.
(c) Assumed potential energy of the jog.

absorption of vacancies. Therefore, the climb of the node may be regarded as the escape of a particle over a potential barrier against a viscous friction. This motion can be treated by the theory of Brownian motion of Kramers[15]. According to him the stationary diffusion current of the probablity finding such a particle is

$$j = \frac{kT}{m} \frac{w \exp\{mV(x)/kT\}\Big|_B^A}{\int_A^B \beta \exp\{mV(x)/kT\}\, dx} , \qquad (2)$$

where m is the effective mass of the jog if the jog is regarded as a particle, β^{-1} the relaxation time of the motion of the jog, w the probability finding a jog and $mV(x)$ the free energy of a jog as a function of its position relative to the nodes A and B. By evaluating the rate of migration of a jog in an infinitely long edge dislocation by an alternate method, and by comparing the rate with that calculated by Kramers' theory we obtain

$$\frac{1}{m\beta} = \frac{4\pi D}{kT} .$$

Assuming the energy required to form a jog at the node A or B be ε_0, we have

$$w = \exp(-\varepsilon_0/kT) .$$

Further we assume

$$mV(x) = \varepsilon_0 + V_0(x) - fb^2x \qquad (3)$$

where

$$V_0(x) \begin{cases} = cx & \text{for} \quad 0 \leq x \leq l_1 \\ = cl_1 & \text{for} \quad l_1 \leq x \leq l - l_1 \\ = c(l-x) & \text{for} \quad l - l_1 \leq x \leq l \end{cases}$$

and

$$\varepsilon_0 + cl_1 = Q ,$$

where l_1 is the effective length of the narrowed part of the extended dislocation by the jog, and Q the energy of a jog in an infinitely long dislocation.

Then it will easily be seen that the integral in (2) may approximately be replaced by $(kT/fb^2) \exp(cl_1/kT)$. Since the quantity $\exp(mV(x)/kT)$ for B would usually be negligible in comparison with that for A, we obtain the frequency of escape of a jog from A to B as

$$P = 4\pi fb^2 \frac{D}{kT} \exp\{-(Q - fb^2l_1)/kT\} \qquad (4)$$

Substituting suitable values into this expression as $D = 10^{-8}\text{cm}^2\,\text{sec}^{-1}$, $T = 1300°\text{K}$, $b = 2.5\times10^{-8}$ cm, $Q = 5$ eV, $l_1 = 10^{-6}$ cm, we obtain

$$P = 10^{-30} f \exp(3.5\times10^{-9} f)\ \text{sec}^{-1}\ \text{dyne}^{-1}\ \text{cm}^2$$

This frequency is too small to cause any significant change in the configuration of the network.

In the above consideration we have neglected the force acting on the node due to the local failure of mechanical balance. Under the action of such forces the activation energy of the jog formation is given as follows:

$$mV(x) = V_0(x) + n(\varepsilon_0 - f'b) - nfb^2x , \qquad (5)$$

(15) H. A. Kramers, Physica, **7** (1940), 284.

where n is the number of atomic planes between the two slip planes, in either of which either side of the dislocation divided by the jog lies respectively, f' the force acting on the node. It will easily be seen from (5) that the activation energy for the formation of jog would vanish, if $f'b$ is greater than ε_0, producing a large jog. It may, therefore, be expected that the frequency of climb of a node is greatly dependent on the force f', which is caused by the local failure of the mechanical balance between line tensions of dislocations.

From the estimation of the line tension it is easily seen that the force f' cannot exceed the critical value when the deformation of the hexagonal network takes place over a few meshes from the free surface or from the annihilating boundary. So if the network could not migrate as a whole, any significant change in the configuration of network would not take place. A dislocation is less mobile in alloys than in pure metal on account of the locking force[16][17]. The mesh of dislocation network is thus smaller in alloy crystals than in pure metals, and its coarsening rate may be neglected when the maximum internal stress due to networks becomes smaller than a fraction of the locking force. After the annealing at a high temperature for a long period the relation may be satisfied by

$$\frac{\beta f_0}{b} \simeq \frac{b\mu}{2\pi l} \qquad (6)$$

where β is a constant with the magnitude of 0.1~0.3, f_0 the locking force. The relation (6) gives a value of the order of 1 micron for the mesh size when f_0/b is 1 kg/mm^2. In pure metals a larger value of l than this may be expected.

In both cases of metals and alloys, if the number of dislocations with the same Burgers vector is far greater than the others, the polygonization takes place. In contrast to the above consideration the polygonization occurs by the interaction between dislocations through their elastic stress as well known[18][19].

If the number of dislocations is greater than a certain value, the dislocations are eliminated by a more effective process, the recrystallization, which we shall discuss in the next.

(ii) Dislocation networks surviving recrystallization

It has been mentioned that a single crystal made by recrystallization method should be almost perfect so far as X-ray studies concerned. Therefore, to study the dislocation networks remaining in recrystallized crystal will give useful knowledges concerning the most resistable ones to be eliminated in otherwise perfect crystal.

The dislocations in a deformed crystal can be divided into two parts, one giving the lattice dilatation and the other the rotation. On the other hand, the recrystallization process is believed to be accompanied by the migration of high energy

(16) A. H. Cottrell, *Strength of Solids* (1948), 30; A. H. Cottrell and B. A. Bilby, Proc. Phys. Soc., **A 62** (1949), 49.
(17) H. Suzuki, Sci. Rep. RITU, **A 4** (1952), 455.
(18) R. W. Cahn, J. Inst. Metals, **76** (1949), 121.
(19) A. H. Cottrell, *Progress in Metal Physics* **I** (London, 1949), 77.

boundaries.[20] It will, therefore, be reasonable to consider that the lattice rotation can be eliminated comparatively easily by those boundary movements. The lattice dilatation caused by some groups of dislocations, which may be of nonrecoverable type of work-hardening[21][22], must need the diffusion of vacancies formed at the boundaries to be eliminated in a new crystal.

Let ρ_1 be the effective number of dislocations giving the lattice dilatation in the volume of L^3 distributed at the same period $2L$ in a deformed crystal, and ρ_0 be that remaining in a new crystal. Then the necessary number of vacancies to be transported in unit time is

$$N_1 = \frac{\gamma L^2}{b} G(\rho_1 - \rho_0) \ , \qquad (7)$$

where γ is the effective number of vacancies corresponding to the dislocation line of one atomic spacing and G the velocity of the boundary migration. At a sufficiently high temperature G in aluminium seems to be given by the form[23]

$$G = a(\rho_1 - \rho_0) W_d D \ , \qquad (8)$$

where a is a constant with the magnitude of 100 cm $\sec^{-1}$ dyne^{-1}, W_d the energy of a dislocation per unit length.

The chemical potential gradient of a vacancy is of course far greater in a strained matrix than in a new crystal, but the vacancy would flow preferentially through the weak field of chemical potential gradient in the new crystal rather than in the strong field of strained matrix, because the vacancy will fall immediately after the formation at the grain boundary into the new crystal on account of the steepest gradient in the normal direction to the grain boundary. Then the concentration gradient of vacancies may be controlled by the stress field remaining in the new crystal.

Meanwhile, the energy of the crystal strained heterogeneously may be released by including a suitable pattern of dislocations. The mean normal stress $\bar{P}$ in the volume giving the lattice dilatation in the new crystal is then related to the number of dislocations by the relation

$$|\bar{P}| = \frac{\gamma \rho_0 b^2}{\kappa} \ , \qquad (9)$$

where κ is the compressibility. The flux of vacancies across unit area in unit time is given in the order by $5D/\Omega \sinh (2\bar{P}\Omega/kT)$,[24] and then the number of vacancies N_2, which comes into the volume of compressed region equal to GL^2 from the expanded one for the elimination of $\rho_1 - \rho_0$ dislocations in unit time, is given as follows:

$$N_2 = L^2(5D/\Omega L) \sinh (2\bar{P}\Omega/kT)$$

or

$$= 10\bar{P}DL/kT$$

(20) P. A. Beck, J. Appl. Phys., **21** (1950), 420.
(21) P. A. Beck, Acta Metallurgica, **1** (1953), 422.
(22) T. Suzuki, Sci. Rep. RITU, **A 1** (1949), 55.
(23) H. Suzuki, Sci. Rep. RITU, **A 5** (1953), 413.
(24) F. R. N. Nabarro, *Strength of Solids*, (1948), 75.

Equating N_2 to N_1, we finally get

$$\frac{(\rho_1-\rho_0)^2}{\rho_0} = \frac{10b^3}{\kappa L a W_d kT} \tag{10}$$

Using the values $\kappa = 1.3\times10^{-12}\,\mathrm{cm^2\,dyne^{-1}}$, $\Omega = 1.7\times10^{-23}\,\mathrm{cm^3}$ for aluminium at $T = 900°\mathrm{K}$ and $L = 5\times10^{-3}\,\mathrm{cm}$, $W_d = 10^{-4}\,\mathrm{erg\,cm^{-1}}$ we get

$$(\rho_1-\rho_0)^2 = 2\times10^7\,\rho_0\,.$$

Since the recrystallization process usually takes place when $\rho_1 > 10^7\mathrm{cm^{-2}}$, it seems to be reasonable to believe that ρ_0 could not decrease less than $10^6\ \mathrm{cm^{-2}}$.

As a result, it may be concluded that the volume dilatation found in a sufficiently large crystal region compared with unit mesh can not perfectly eliminated during recrystallization process. Such stress fields remaining in a crystal will induce certain consistent arrangements of dislocation networks. The simplest one answering this is, for instance, the 'honeycomb' structure as already shown in Fig. 4. In this structure, the hexagonal axis is parallel to the normal of the vector plane, and plane networks in the prism surfaces are of {112} type, resulting from a slight rotation around the screw axis of the regular {113} network. These screw dislocations meet at the nodes in the boundary, where three plane networks meet. The boundary between such honeycomb structures of different schemes would be filled by other space networks, for instance, such as formed in the surfaces of orthic-tetrakaidecahedron already discussed.

IV. Comparison of the theory with experiments

1. Hedges and Mitchell's observation[2]

During the investigation of latent images in a transparent silver-bromide single crystal, they have succeeded in making dislocation lines visible by the separation of photolytic silver along them. Their observations indicate that the dislocation networks are, in fact, distributed in boundaries between adjacent elements of polyhedral substructures.

The regular patterns of particles of photolytic silver (Fig. 2 and 3 in the paper quoted) are likely indicating that the present picture of the space arrangement of the dislocation networks shows a fairly good accordance with real one. Fig. 2 indicates clearly the hexagonal plane networks and Fig. 3 shows certain polyhedral networks or hexagonal ones.

Their results were obtained in crystals at 'polygonization' state, that is, at an intermediate stage to form dislocation networks in polyhedral surfaces and to settle them in a mechanical balance. It must be stressed, however, that those patterns of dislocations quoted form the sub-boundaries between blocks of relatively perfect crystal across about several ten microns.

2. X-ray reflexion

The present picture of the dislocation networks in an annealed crystal leads us to the conclusion that the estimation of the density of dislocations by X-ray method should be modified in some essential points and that the model of 'mosaic' blocks

introduced by Darwin to explain the intensity of X-ray reflexion from imperfect crystals can be expressed more in rigour and more in concrete than before.

The width of reflexion determined by Guinier and Tennevin[25] for relatively perfect aluminium crystals and later by Gay, Hirsch and Kelly[26] show the range of misorientation within grain about 0.1 cm across to be only 30″ to 1′.

Consider a uniform distribution of polyhedral domains of L^3 in volume, each of which is surrounded by plane networks of dislocations as shown in Fig. 6.

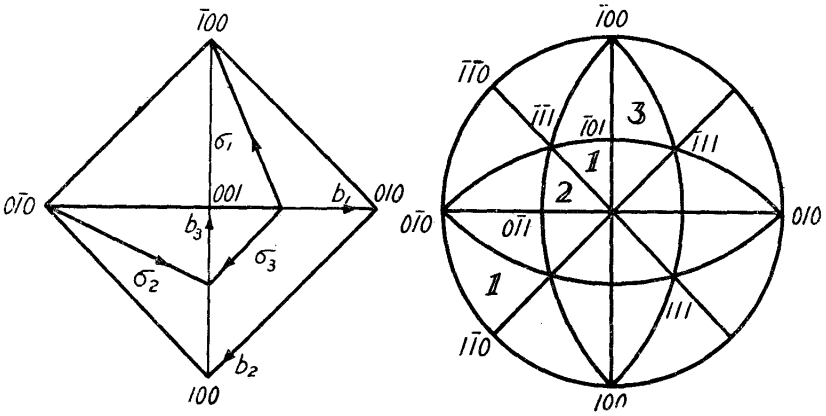

Fig. 6. Illustration of $(\bar{1}\bar{1}3)$ network.

There are thus d/L domains in the distance of d, and each domain is assumed to give an angle deviation of $\delta\theta$ with the same probability independent of its sign. The probability of producing a misorientation of θ within d cm is

$$W(\theta) = \frac{2^{d/L}}{(2\pi \frac{d}{L}\delta\theta^2)^{\frac{1}{2}}} \exp\left(-\theta^2/2\,\frac{d}{L}\delta\theta^2\right) \tag{11}$$

For a relatively small value, $\bar{\theta}$ is given in good approximation by

$$\bar{\theta} = \sqrt{\frac{d}{L}}\,\delta\theta \tag{12}$$

The appropriate substitution by arrays of edge dislocations for $\{112\}$ networks is made. Putting the mean spacing of n dislocations h, it becomes $\delta\theta \simeq b/h$ and $L=nh$. Thus we get $\bar{\theta} = \sqrt{\frac{d}{nh}}\,\frac{b}{h}$. Using the reasonable values $b=3\times10^{-8}$cm, $h=5\times10^{-4}$ cm and $n=10$, $\bar{\theta}$ is obtained for $d=0.1$ cm as follows: $\bar{\theta}=2.7\times10^{-4}\sim1'$. This is well in accordance with X-ray results for relatively perfect metal crystals quoted before.

An important point to be remarked concerns the usual estimation of coherent domain size by X-ray reflexion. Dislocations forming a network are considered to yield some subsidiary mosaics so far as X-ray reflexion is concerned, each of which is defined by a single dislocation. In fact, the estimation of the size of a coherent domain has been interpreted to be the same as that of 'mosaic' block. The size of mosaic block in most crystals was thus mistaken to be about one micron in average.

(25) A. Guinier and J. Tennevin, Comptes Rendus, **226** (1948), 1953.
(26) P. Gay, P. B. Hirsch and A. Kelley, Acta Metallurgica, **1** (1953), 315.

The conventionally accepted density of dislocations in an annealed crystal is also in error, because of the assumption that dislocation arrays form the mosaic wall of about one micron in linear size. This is the case for the assumption that dislocations are uniformly distributed throughout a crystal.

The density of dislocations in an annealed crystal was found from the present picture to be about 2×10^6 cm/cm^3 by using the values already quoted.

3. Etch-pattern

The most powerful method of determining directly the pattern of dislocation networks in metal crystals is likely to be a delicate etch-pit method. It has been found, in fact, to be very useful tool to test the dislocation model of crystal sub-boundaries by Lacombe[27] on aluminium and later by Vogel et al[28] on germanium.

Along this line, one of the present authors studied thermal etch-patterns in α-brass single crystals[29] produced under appropriate conditions. Under such conditions we can make a smaller rate of the lattice diffusion of zinc atoms than that of the vapourization. Thus, a short-cut diffusion of those atoms along the dislocation lines can take place preferentially. As a result, pits will refer to the dislocation ends.

In fact, we confirmed the number of etch-pits equal to that of excess dislocations from the observation of a crystal deformed by a pure bending with the radius of curvature as small as 1.5 mm, which corresponds to about 3×10^8 lines of dislocations in unit area.

Though the details of this experiment will be reported elsewhere, the result was less convincible concerning the space arrangements of dislocation networks. It may come from certain changes in the local balance between line tension of dislocations due to the appearence of new free surface. Nevertheless, etch-patterns in annealed α-brass crystals lead to the conclusion that the density of dislocations is about $10^7\sim10^8$ lines/cm^2. We have other knowledges to believe that dislocation density in alloy crystals is, in general, larger than that in high purity metal as already mentioned.

Forty and Frank[30] have recently developed a fine technique to obtain etching-pits showing every dislocations in high purity aluminium. According to the lecture made by Frank in Nikko Symposium, such observations never supported the view that there was a lower limit of dislocation density of the order of 10^8 cm/cm^3. His conclusion is just the same as the prediction given by the present authors.

Imura and one of the present authors[31] have recently succeeded to show that the honeycomb structure mentioned above really exists in a face-centered cubic crystal of Al-Mn alloys.

---

(27) P. Lacombe, *Strength of Solids*, (1948), 91.
(28) F. L. Vogel, W. G. Pfann, H. E. Carey and F. E. Thomas, Phys. Rev., **90** (1953), 489.
(29) H. Suzuki, to be published.
(30) A. J. Forty and F. C. Frank, read at Nikko Simposium on Dislocation Plasticity (1953), to be published.
(31) T. Suzuki and T. Imura, read at International Conference on Defects in Crystals held at Bristol on July 1954, to be published.

V. Motion of dislocation network

1. Characteristic matrix associated with dislocation networks

When a line dislocation with Burgers vector $\boldsymbol{b}$ moves in a plane $\boldsymbol{n}$, a given atom in the position (x, y, z) moves macroscopically to the new one (x', y', z'), that is,

$$\begin{pmatrix} x' \\ y' \\ z' \end{pmatrix} = \begin{pmatrix} 1+b_xn_x & b_xn_y & b_xn_z \\ b_yn_x & 1+b_yn_y & b_yn_z \\ b_zn_x & b_zn_y & 1+b_zn_z \end{pmatrix} \begin{pmatrix} x \\ y \\ z \end{pmatrix}. \tag{13}$$

The vector $\boldsymbol{n}$ has the magnitude equal to the area swept by the dislocation and is normal to that area.(32)* If the respective deformations due to the motion of a number of dislocations are so small that they can be summed up independently, it will become

$$\begin{pmatrix} x' \\ y' \\ z' \end{pmatrix} = (\|e\| + \|D\|) \begin{pmatrix} x \\ y \\ z \end{pmatrix}, \tag{14}$$

where

$$\|e\| = \begin{pmatrix} 1 & 0 & 0 \\ 0 & 1 & 0 \\ 0 & 0 & 1 \end{pmatrix}$$

and

$$\|D\| = \begin{pmatrix} \sum_i b_{ix}n_{ix} & \sum_i b_{ix}n_{iy} & \sum_i b_{ix}n_{iz} \\ \sum_i b_{iy}n_{ix} & \sum_i b_{iy}n_{iy} & \sum_i b_{iy}n_{iz} \\ \sum_i b_{iz}n_{ix} & \sum_i b_{iz}n_{iy} & \sum_i b_{iz}n_{iz} \end{pmatrix} \tag{15}$$

Consider a parallel displacement of dislocation networks equal to $\boldsymbol{s}$. Then it must satisfy the following relation:

$$\boldsymbol{n}_i = \int_{\sigma_i} \left(\frac{d\vec{\sigma}_i}{d\sigma_i} \times \boldsymbol{s} \right) d\sigma_i \tag{16}$$

Here $\vec{\sigma}_i$ is the i-dislocation line and σ_i its length. Since the dislocation bent between nodes can be substituted by the line with no effect on a macroscopic deformation, we use a simple expression in place of Eq. (16), namely,

$$\boldsymbol{n}_i = \vec{\sigma}_i \times \boldsymbol{s}$$

Thus, Eq. (15) can be written in the following form:

$$\|D\| = \begin{pmatrix} V_{xx} & V_{yx} & V_{zx} \\ V_{xy} & V_{yy} & V_{zy} \\ V_{xz} & V_{yz} & V_{zz} \end{pmatrix} \begin{pmatrix} 0 & -s_z & s_y \\ s_z & 0 & -s_x \\ -s_y & s_x & 0 \end{pmatrix}, \tag{17}$$

where the relation $V_{lm} = \sum_i b_{il}\sigma_{im}$ is used.

As the result, the deformation due to the movement of dislocation network can be given by operating the matrix depending only on the direction of displacement

(32) H. Suzuki, Sci. Rep. RITU, **A 6** (1954), 30.

* The signs of $\boldsymbol{b}$ and $\boldsymbol{q}$ (equal to $\boldsymbol{n}$ here qeuoted) are discussed in reference to Fig. 6 and Table 1.

upon the matrix characteristic of the network considered.

The work done by the external stress $\|F\|$ is, therefore,

$$W = \sum_j \sum_i F_{ij} D_{ij} \tag{18}$$

2. Motion of dislocation nodes

It must be remembered that three dislocations meeting at the node in a regular {113} network can not glide on the respective slip planes at the same time so as to displace the node. Accordingly, an unit process for the motion of three-fold node is resulted from (a) two dislocations glide first and then the rest climbs, or from (b) only one glides and the two others climb*.

The activation energies for those processes are of the same order. As for the magnitude of displacement of a given node, however, (a) gives $\frac{a}{2}<110>$ while (b) is $\frac{a}{2}<211>$. From this point alone it permits the process (b) to be more favoured than (a). In the following, we will make some calculations following this supposition, but we can find that the case (a) will give nearly the same result.

Table 1 and Fig. 6 give various quantities and notations referring to $(\bar{1}\bar{1}3)$ network appearing in the following calculation. Here $\boldsymbol{q}$ defines the positive side of slip plane in which an excess half-plane is inserted to give a specified edge dislocation, and $\boldsymbol{q} = \vec{\sigma} \times \boldsymbol{s}$. We also define the Burgers vector of a dislocation line following the mode of Frank[7]. To decide the direction $\boldsymbol{s}$ of glide movement of a dislocation, the formal treatment is based on that of Thompson[9].

Table 1. Some notations used in the following calculation in reference to $(\bar{1}\bar{1}3)$ network.

	Burgers vector $\boldsymbol{b}$	Dislocation line $\vec{\sigma}$	Normal to slip plane $\boldsymbol{q}$	Direction of displacement of node $\boldsymbol{s}$
Edge 1	$\frac{a}{2}[01\bar{1}]$	$[\bar{2}\bar{1}\bar{1}]$	$[1\bar{1}\bar{1}]$	$\frac{s_0}{\sqrt{6}}[12\bar{1}]$
Edge 2	$\frac{a}{2}[\bar{1}01]$	$[121]$	$[1\bar{1}1]$	$\frac{s_0}{\sqrt{6}}[21\bar{1}]$
Screw 3	$\frac{a}{2}[1\bar{1}0]$	$[1\bar{1}0]$	—	$\frac{s_0}{\sqrt{6}}[112]$

Here, $s_0=\sqrt{3}b, a=\sqrt{2}b$, b the strength of perfect dislocation and a the lattice constant.

The velocity and the direction of the displacement of a node is given by the summation of the frequency of a unit process (b) times the amount of unit displacement, since each process can be assumed to be independent of another on account of the relatively slow velocity of the process considered.

Now consider the case, where j-dislocation glides by unit distance to give the displacement $\boldsymbol{s}_j$ of a given node. Since the force acting at a node comes only through dislocation lines meeting there, the work done during the unit process

* The term 'climb' is used here to denote the motion of a dislocation in the direction of the normal to the silp plane, in which the dislocation is dissociated into two partials.

considered is given by $\sum_i E(\vec{\sigma}_{i0}\cdot\boldsymbol{s}_j)$, where E is the line tension of dislocation ($\sim\mu b^2/2$) and $\vec{\sigma}_{i0}$ line vector of i-dislocation in the vicinity of the node.

Then, the frequency of migration of the node in the direction $\boldsymbol{s}_j$ is given by

$$\nu\left[\exp\left(-\{U-E\sum_i(\vec{\sigma}_{i0}\cdot\boldsymbol{s}_j)\}/kT\right)-\exp\left(-\{U+E\sum_i(\vec{\sigma}_{i0}\cdot\boldsymbol{s}_j)\}/kT\right)\right]$$

$$\simeq\nu\frac{2E}{kT}\sum_i(\vec{\sigma}_{i0}\cdot\boldsymbol{s}_j)\mathrm{e}^{-U/kT},$$

where U is the activation energy of the unit process considered. It is, e.g., given by the sum of the energies of the two jogs and the migration energy of vacancy in a somewhat strained region near the node.

From this we get the velocity of the node migration $\boldsymbol{v}$ as follows:

$$\boldsymbol{v}=\nu\sum_j\boldsymbol{s}_j\frac{2E}{kT}\sum_i(\vec{\sigma}_{i0}\cdot\boldsymbol{s}_j)\,\mathrm{e}^{-U/kT}, \tag{19}$$

where ν is of the order of the jump frequency of atom.

Now, $\vec{\sigma}_{i0}$ can be divided into two parts, e.g., $\boldsymbol{q}_i$ and $\boldsymbol{p}_i$. The former is referred to the normal component and the latter the parallel one regarding the glide plane. Thus, the work done during the unit process considered is divided into the corresponding two parts:

$$E\sum_i(\vec{\sigma}_{i0}\cdot\boldsymbol{s}_j)=E\sum_i(\boldsymbol{p}_i\cdot\boldsymbol{s}_j)+E\sum_i(\boldsymbol{q}_i\cdot\boldsymbol{s}_j). \tag{20}$$

It must be noted that $E\cdot\boldsymbol{p}_i$ is equal to one half of the external force acting on i dislocation plus a certain balance force at the node. So we get

$$W_j=2E\sum_i(\boldsymbol{p}_i\cdot\boldsymbol{s}_j) \tag{21}$$

From Eqs. (19), (20) and (21), the displacement velocity is finally given by

$$\boldsymbol{v}=\frac{\nu}{kT}\left\{\sum_j W_j\boldsymbol{s}_j+2E\,s_0{}^2\sum_i\boldsymbol{q}_i\right\}\mathrm{e}^{-U/kT}. \tag{22}$$

At a steady-state of motion of nodes, vacancies must be created and absorved steadily along each dislocation. Putting the rate of the formation of vacancies on the j-dislocation $\dot{n}_j$,

$$\dot{n}_j=\frac{1}{\Omega}(\boldsymbol{b}_j\cdot\vec{\sigma}_j\times\boldsymbol{v}). \tag{23}$$

It may be reasonably assumed that the formation of vacancies along the screw dislocation will be cancelled by the annihilation of them along the same line, and so we get

$$\dot{n}_3=0 \tag{24}$$

This assumption is also supported by the supposition that the screw elements in a given network are sufficiently shorter than the edge ones. Since it must hold that $\sum\dot{n}_i=0$ at a steady-state, and that the vacancy currents flow mainly between the neighbouring edge dislocations, the long-distance diffusion may be neglected;

so it becomes

$$\dot{n}_1 = -\dot{n}_2 \tag{25}$$

Here, we confine the discussion in the case in which the edge dislocation 1 belongs to the operative system decided by externally applied tensile stress. In this case, the vacancy flows from 1 to 2.

If these assumptions are valid, the direction of displacement of the node should be given by

$$\boldsymbol{\nu} = [x\,x\,1]\frac{v}{\sqrt{2x^2+1}} \tag{26}$$

Putting the length of the dislocation as $l = l_1 = l_2$, we get from (23) and (26)

$$\dot{n}_1 = \frac{v\,l\,b}{\Omega\sqrt{3}\,\sqrt{2x^2+1}} \tag{27}$$

Using Eq. (26), we can write the x, y, z components of $\boldsymbol{\nu}$ from Eq. (22). After a short calculation, it becomes

$$\frac{x\,v}{\sqrt{2x^2+1}} = \frac{b}{2\sqrt{2}}\frac{\nu}{kT}(3W_1 + 3W_2 + 2W_3)\,\mathrm{e}^{-U/kT} \tag{28}$$

and

$$q_2 = \frac{W_1 - W_2}{2\sqrt{6}\,E} - q_1\,. \tag{29}$$

Thus, we get the migration velocity of a given network as a function of x.

The next problem is to obtain q as a function of x. Let r_i be the normal component of the radius of curvature of i-dislocation referring to its glide plane. Then, it becomes $q_i = l/r_i$. When we assume the uniform distribution of jogs, the avarage spacing between them is given by

$$\Delta \simeq 8\sqrt{\frac{2}{3}}\,br_1/l. \tag{30}$$

Therefore, q_i gives us the knowledge concerning the radius of curvature of the dislocation or the number of jogs along it. Since the activation energy is needed for the formation of vacancy at a jog but not for the absorbtion, the normal flux of vacancies is

$$\dot{n}_1 = \frac{l}{\Delta}\nu\left(\mathrm{e}^{-\frac{W_f' + W_m'}{kT}} - c_1\,\mathrm{e}^{-\frac{W_m'}{kT}}\right), \tag{31}$$

where W_f and W_m are the activation energies for the formation and the migration of vacancy, respectively. W_f' and W_m' correspond to those energies at a jog. The second term is due to the vacancies flowing back from the crystal region in the neighbourhood of the source, where the concentration is given by c_1. Since we can give the substitution as $\delta W_f = W_f - W_f' = -Eb/r_1$, by using the relation (30) Eq. (31) can be written as

$$-\dot{n}_1 = \frac{\sqrt{3}}{8\sqrt{2}}\frac{l^2}{b}\frac{1}{r_1}\frac{\nu}{kT}\left(\frac{Eb}{r_1} + kT\ln\frac{c_1}{c_0}\right)\mathrm{e}^{-W/kT}, \tag{32}$$

where we put $c_0 = \mathrm{e}^{-W_f/kT}$ and $W = W_f + W_m$.

On the other hand, imagine the parallel filaments of source and sink at a distance

equal to L. L is to be written only by l in this model concerning the plane network. Then, it follows

$$\dot{n}_1 = \pi D_m l (c_1 - c_2) / \Omega \ln \frac{L}{b} , \tag{33}$$

where l is the length of those filaments, and D_m the migration velocity of vacancy. c_1 and c_2 are respectively the concentrations along them. Using the relation $Eb/r_2 \sim kT(1-c_2/c_0)$, we can eliminate c_1 and c_2 from (32) and (33). Then, it follows

$$\dot{n}_1 = \frac{3\sqrt{3}}{8} \frac{E}{kT} \frac{bD_m c_0}{\Omega} (q_2 - q_1) q_1 , \tag{34}$$

assuming that $q_1 \ln \frac{L}{b} \ll 1$

After the elimination of q_2 from Eq. (34) using Eq. (29), and inserting for v the relation given by Eq. (27) and (28), the final equations concerning x and q_1 are obtained, e.g.,

$$\left.\begin{aligned} y &= -\eta + \frac{\xi}{x} \\ y &= \zeta - \frac{(\eta + \zeta)\phi}{\sqrt{3x^2 + 6x + 5}} \end{aligned}\right\} , \tag{35}$$

where

$$\left.\begin{aligned} y &= 64\sqrt{6} \frac{f}{F} \frac{b}{l} \beta \\ f &= 2 \frac{E}{b^2 l'} = \frac{\sqrt{3}}{4\sqrt{2}} \frac{E}{\beta b^3} q_1 , \end{aligned}\right\} , \tag{36}$$

and

since

$$l' = \beta \Delta \simeq 8\sqrt{\frac{2}{3}} \beta b / q_1 .$$

Parameters in (35) are respectively as follows:

$$\left.\begin{aligned} \xi &= \frac{2\sqrt{6}}{Fb^2 l} (3W_1 + 3W_2 + 2W_3) \\ \eta &= \frac{2\sqrt{6}}{Fb^2 l} (W_1 + 3W_2 - 4W_3) \\ \zeta &= \frac{2\sqrt{6}}{Fb^2 l} (W_1 - W_2) \\ \phi &= \frac{\sqrt{3}}{\pi} \frac{l}{b} \ln \frac{L}{b} e^{-\frac{U-W}{kT}} \end{aligned}\right\} \tag{37}$$

The significance of the substitution made in Eqs. (36) will clearly be understood. Let l' be the effective length of the dislocation which decide a critical shear stress for slip in the sence of Frank and Read[3]. Then, the critical shear stress f is given by $2E/b^2 l'$. Since the dislocation is dissociated into partials, at lower temperatures the jogs may tend to gather to decrease the line energy as far as possible. The unknown distribution of the jogs, thus, makes it difficult to estimate precisely l' or β. It is, however, certain that at least the jogs comparatively near the nodes play a role in the increase of the critical stress for the multiplication by shortening the effective length of dislocation.

Important points to be noted are the hardening effect introduced at just discussed and the possiblity of an alternative mechanism for the slow rate creep whose rate varies linearly with the applied stress, being zero only at zero load as proposed dy the present theory. The orientation dependence of the 'micro-creep hardening' predicted first by the present theory is obtained after some calculations as shown in Appendix of this report, which gives y in (35) as a function of crystallographic orientation of specimen axis parallel to the tensile stress.

VI. Relation of theory to experiment concerning micro-creep and the related phenomena in face-centred cubic crystals

It has been found[33] that the micro-plasticity of copper and aluminium single crystals showed different behaviours in certain important respects from that of tin crystal observed by Chalmers.[34] The main characteristics of the micro-creep in face-centred cubic crystals were as follows: (a) It was composed of two stages, say, the initial and the steady-state. Both creep rates increased linearly with externally applied stress and was zero only at zero load. The former rate was about a hundred times larger than that of the latter. (b) The activation energy for the steady-state creep for copper crystals was about 40 kcal/mol^{-1}, which was of the same order of that for selfdiffusion. (c) Once the micro-creep proceeded at a given stress, the change to another larger stress altered a part of the character mentioned in (a). The initial creep was exhausted. That is to say, such a change in stress just as mentioned gives always little initial creep but a steady-state micro-creep corresponding to a new stress e.g., only a steady-state micro-creep is independent of the hystory. (d) Remarkable hardening effect was observed. Even though there was found to be a sharp yield point in so far as the stresses were always applied to virgin crystals, the change in external stress in the sense of what mentioned in (c) or the stress increment at a slow constant rate such as 1 gr mm^{-2}hr^{-1} gave nó yield point and the creep continued at a given steady-state rate as in (c). (e) Micro-creep rate and its hardening was found to depend on the crystallographic orientation of crystal examined.

The most remarkable point in this case is the fact that no saturation was observed for the steady-state micro-creep. Further, the results (d) and (e) are actually new facts.

Before we apply the present theory to the micro-creep of a face-centred cubic crystal, the theory proposed by Cottrell and Jaswon[35] must be examined. After some calculations,[36] however, the creep rate given by some mechanism similar to Cottrell's proposal is found to be so large that it differs from the observed values by the factor of about 100, e.g., $\frac{ds}{dt} > 10^{-6}\,\mathrm{sec}^{-1}$ at 500°C for a copper crystal. Observed values for the initial creep rate, however, are almost of the same order.

(33) T. Suzuki, to be published.
(34) B. Chalmers, Proc. Roy. Soc., **A 156** (1936), 427.
(35) A. H. Cottrell and M. A. Jaswon, Proc. Roy. Soc., **A 199**, 104.
(36) H. Suzuki, to be published.

As a result, the present theory becomes very attractive at least for the steady-state micro-creep and the phenomena concerning micro-creep hardening observed at relatively high temperatures. It must be remembered, however, that the interaction between plane networks is not taken into account at all. To explain such an amout of total creep strain as $10^{-4}\sim10^{-5}$ examined in most cases, it is necessary to examine a certain effect of constraint given at the junctions of plane networks, even if their collision with one another can be neglected.

The first doubt cast on the micro-creep mechanism is, thus, whether micro-creep should be explained by somewhat similar mechanism to give a diffusional viscosity in polycrystal as discussed by Nabarro,(24) Herring(37) and Ookawa(38) or not. In the present case, the 'boundary' means, of course, the network in certain polyhedral surfaces imagined. This possibility is out of scope from the present theory, which assumed that the vacancy current must be short-distance in nature, $\sum_i \dot{n}_i = 0$. Those vacancies, if any, are supposed to be a small fraction of ones playing a role in the short distance diffusion considered. It is important to note that the orientation dependence of micro-creep is probably difficult to be explained by this mechanism alone.

So far as each regular plane network occupies a relatively large area, most parts of the network move to a specified direction as the theory predicted. Dislocations near the junctions with other networks are thus forced to increase their length owing to the considered in general case. Then, the flux of vacancies rapidly in those parts, but soon it must cease to change by branching of dislocations as illustrated in Fig. 7 by dotted lines. Besides, the multiplication of free dislocation loops is interrupted because of a number of jogs along the dislocations considered.* From this supposition the model concerning the displacement of dislocation networks may give a right explanation for the micro-creep.

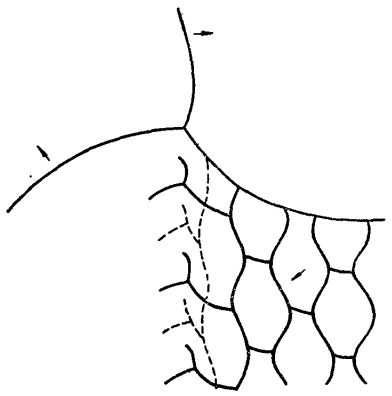

Fig. 7. Some change in the configuration near the boundary of plane networks associated with their migration.

1. Micro-creep rate of face-centred cubic metals

From the present theory the micro-creep rate is deduced from Eq. (27). When $\phi > 1$, which will be justified later, it becomes $|x| > 1$. So we get approximately $\left|\frac{x}{\sqrt{2x^2+1}}\right| \simeq \frac{1}{\sqrt{2}}$. Thus, the velocity of migration of the dislocation network is given by

$$v = \frac{b}{2}\frac{\nu}{kT}|3W_1 + 3W_2 + 2W_3|e^{-U/kT}.$$

Using (37), it becomes

(37) C. Herring. J. Appl. Phys., **21** (1950), 437.

(38) A. Ookawa, Kobayashi Rikagaku-kenkyujo-hokoku, **1** (1951), 255. (in Japanese).

* The coarsening of the network is neglected.

$$v = \frac{Fb^3 l}{4\sqrt{6}} \frac{\nu}{kT} |\xi(\theta, \varphi, \alpha)| e^{-U/kT} .$$

Inserting the values, $l = 10^{-4}$ cm, $\nu = 10^{13}$sec^{-1} and $T = 700$°K, which gives $v = 0.02 F\xi|(\theta, \varphi, \alpha)|e^{-U/kT}$, where F is the tensile applied stress. After a short calculation (see Appendix), $|\xi|$ is found to be of the order of 10. Thus, we get

$$v = 0.4 FD e^{-\frac{U-W}{kT}} .$$

Here we put $D = 0.5e^{-W/kT}$ as the self-diffusion coefficient.

Since $U-W$ is of the order of 1,000 cal mol^{-1} as discussed in the following, the order of v is obtained as

$$v = 0.2FD \tag{38}$$

The tensile micro-creep rate at a steady-state $\dot{s}$ is given as follows:

$$\dot{s} = 5\times10^{-2} \rho bFD , \tag{39}$$

where ρ is the density of dislocations whose order is 2×10^6 cm^{-2} from the earlier estimation. When we deduce v from (38), we must take an appropriate average of v over the possible networks. In this sense, $\dot{s}$ obtained from (39) shows the upper limit. Putting $F = 10^6$ dynes cm^{-2}, $D \simeq 10^{-12}$ cm^2 sec^{-1} and $b \simeq 3\times10^{-8}$ cm, it gives

$$\dot{s} \simeq 3\times10^{-9} \text{ sec}^{-1} .$$

Experimentally, $\dot{s} = 1.5\times10^{-9}$ sec^{-1} at 400°C; 3×10^{-8} sec^{-1} at 500°C; 20×10^{-8} sec^{-1} at 550°C, under the application of stress just below yield point. Thus those results show a fair agreement with the theory.

2. Micro-creep hardening (Stress-annealing effect on stress-strain curves)

The degree of micro-creep hardening can be estimated from y in Eq. (37). For this aim it is nesessary to eliminate x from the two equations and to know the magnitude of ϕ. Assume $l_s \ll l$ and then it becomes $\alpha \ll 1$ and putting $L = \frac{1}{4} l = \frac{1}{4}\times10^{-4}$ cm and using the earlier estimations, we get

$$\phi = 2\times10^4 e^{-\frac{U-W}{kT}} .$$

U is slightly larger than two times the activation energy for the formation of a jog at a node as described before. If we assume that the formation energy of a jog is about one half of that for normal place along dislocation, it becomes $U \leq 4$eV. On the other hand, W is of the order of 2.8 eV according to Huntington and Seitz.[39] Thus, it is reasonably supposed to be $U > W$. The following values show the relation between ϕ and $U-W$ deduced from the above equation.

$U-W$ in cal mol^{-1}	1,000	4,000	16,000
ϕ	10,000	2,000	5

According to the experimental determination of $U-W$ from the temperature dependence of f/F on crystals with the same orientation, $U-W$ is about 1,000 ~3,000 cal mol^{-1}.

(39) H. B. Huntington and F. Seitz, Phys. Rev., **61** (1942), 345.

From this we may take as $\phi \gg 1$. According to Eqs. (35) and (37), the absolute value of y is found to increase with ϕ. After the numerical calculation (see Appendix), it becomes $0 \leq |y| \leq 10$. Numerical values of y are sterographically plotted as a function of crystallographic direction of the tension axis in Fig. 8.

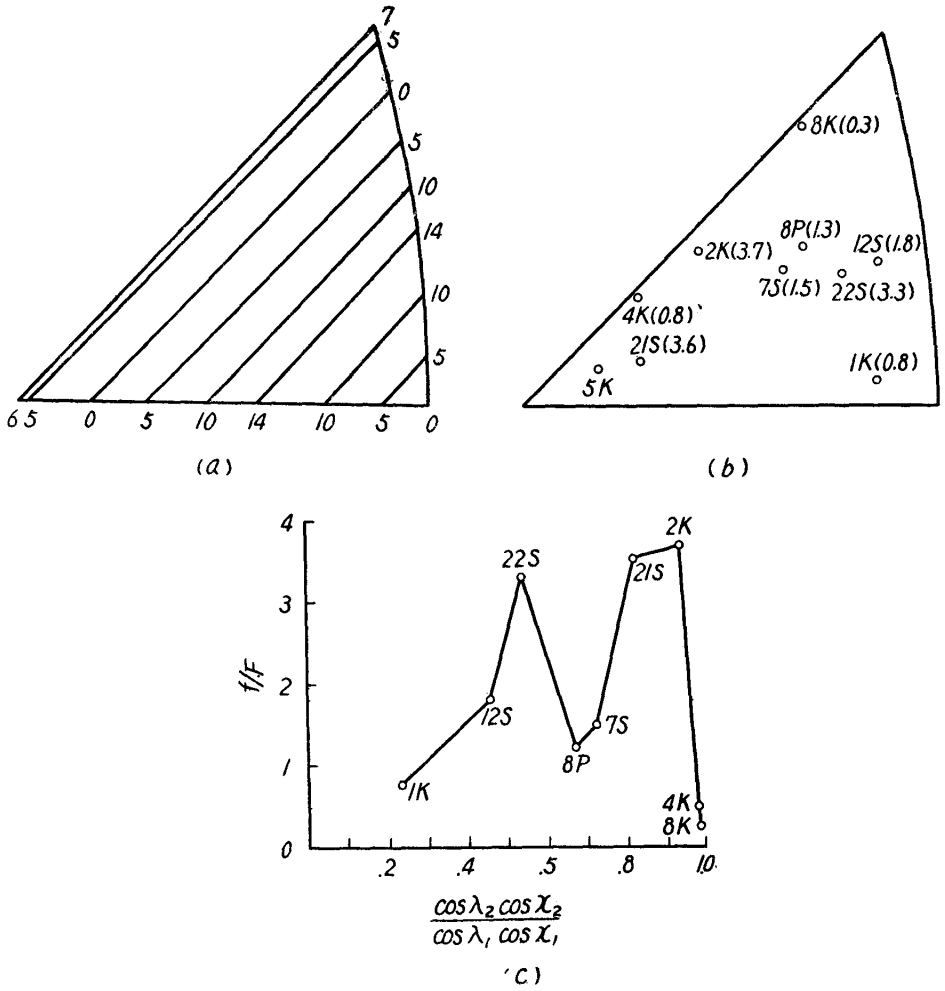

Fig. 8. (a) Numerical values of y as a function of tension axis when $d \gg 1$. (b) Experimental results concerning the stress-annealing effect (f/F) for aluminium crystals. (c) f/F as a function of the ratio of the direction factor of the slip system 2 to the operative one. Here it must be noted that

$$\frac{\cos\lambda_2 \cos\chi_2}{\cos\lambda_1 \cos\chi_1} + \frac{\cos\lambda_3 \cos\chi_3}{\cos\lambda_1 \cos\chi_1} = 1,$$

where the suffixes referred to Fig. 6, (c). λ_i is the angle between the tensile axis and the slip direction of the i-th slip system, and χ_i the angle between the tensile axis and the slip plane of the i-th slip system.

Two triangles in the figure of standard stereographic projection are obtained as the slip systems corresponding to the edge dislocation 1. The attention should be paid on the system to give a lower critical stress. Thus, folding two triangles on each other, lower values of y are plotted in Fig. 8(a). Experimental values of f/F for aluminium crystals are shown in the same figure (b) and (c), where f is the critical shear stress at room temperature and F the tension stress applied during

annealing at 350°C. for one day long. Not coming into fine details, both are in fair agreement with each other. Here, it must be rememberd that the effect of 'stress-anneal' decreases abruptly in the neighbourhood of <100> – <111> boundary as observed in experiments. This is probably explained by the prediction that on that boundary the displacement of dislocation nodes considered can not occur, because of equal mobility of edge dislocations 1 and 2.

From Eq. (35), using $0 \leq |y| \leq 10$, it becomes

$$0 \leq f/F \leq l/15\beta b \simeq 200/\beta$$

It is difficult to estimate the order of β as discussed before, but it may be safe to take as $\beta \simeq 10$. Then, it gives

$$0 \leq f/F \leq 20 \tag{40}$$

Experimentally we get $f/F \leq 4$. Taking into account of some ambiguity in the order of β, we must satisfy with these results. An example of experimental results is shown in Fig. 9.

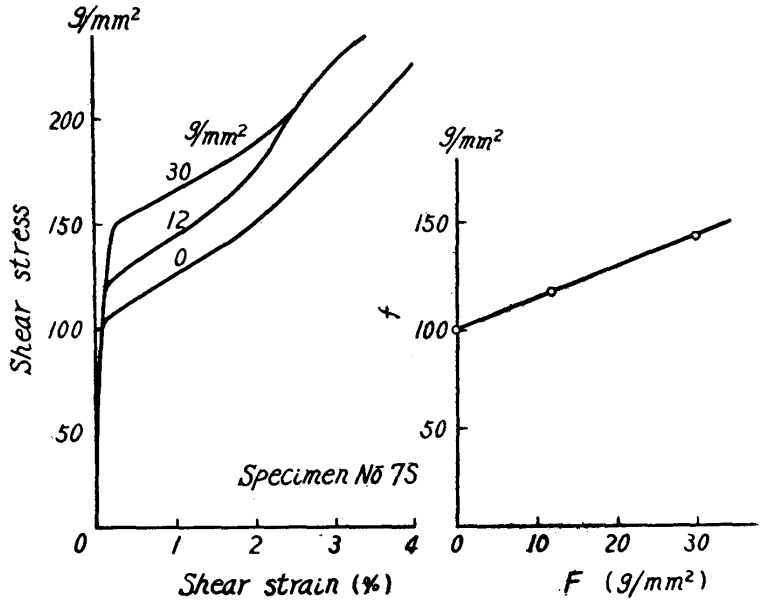

Fig. 9. An example of the effect of stress-annealing on stress-strain curve of high purity aluminium crystal.

The theoretical estimation as given by Eq. (40) seems also to be very useful to slove the subjects concerning the variation of critical shear stress owing to nuclear irradiation at least in its initial stages. According to Blewitt[40], the critical shear stress of copper crystal increased from 0.241 to 2.0 kg mm^{-2} for a fast neutron flux of about 2×10^{18} *nvt*. The production of displaced atoms, e. g., vacancies and interstitials is expected to displace the dislocation networks in a similar way but irregularly as in the micro-creep induced by the application of external stress before they condense to form somewhat larger clusters.

Acknowledgements

We wish to thank Professors M. Yamamoto and S. Takeuchi for their continued interest and support for our work, and our collaborators in our laboratory for valuable discussions and helps for the preparation of this manuscript.

Appendix

Let n be the plane defined by a given tensile axis and [100] direction. φ can

(40) T. H. Blewitt and R. R. Coltman, Phys. Rev., **82** (1951), 769 A.

be defined as the angle between $\boldsymbol{n}$ and (010) plane, and θ as the one between the tensile axis and (100). Then, we can write a tensile stress F into components as a function of θ and φ as follows:

$$\|F\| = F\begin{pmatrix} \sin^2\theta & -\sin\theta\cos\theta\sin\varphi & \sin\theta\cos\theta\cos\varphi \\ -\sin\theta\cos\theta\sin\varphi & \sin^2\varphi\cos^2\theta & -\cos^2\theta\sin\varphi\cos\varphi \\ \sin\theta\cos\theta\cos\varphi & -\cos^2\theta\sin\varphi\cos\varphi & \cos^2\theta\cos^2\varphi \end{pmatrix}$$

In a given network, we put the ratio of the length of the screw dislocation l_s to that of the edge one to be $l_s/l = \sqrt{3}\,\alpha$. The macroscopic deformations $\|D\|$ are given by Eq. (17) as follows:

$$\|D_1\| = \frac{b^2 l}{2\sqrt{6}}\begin{pmatrix} 4+\alpha & -2+\alpha & 3+\alpha \\ 3-\alpha & -3-\alpha & -3-3\alpha \\ -7 & 5 & 3 \end{pmatrix},$$

$$\|D_2\| = \frac{b^2 l}{2\sqrt{6}}\begin{pmatrix} 3+\alpha & -3+\alpha & 3+3\alpha \\ 2-\alpha & -4+\alpha & -3\alpha \\ -5 & 7 & -3 \end{pmatrix},$$

$$\|D_3\| = \frac{b^2 l}{2\sqrt{6}}\begin{pmatrix} -3-2\alpha & 1-2\alpha & 1+2\alpha \\ -1+2\alpha & 3+2\alpha & -1-2\alpha \\ 4 & -4 & 0 \end{pmatrix},$$

Inserting those expressions, W_1, W_2 and W_3 are respectively obtained from Eq. (18) as a function of θ,φ and F. Thus, parameters ξ, η and ζ in Eq. (37) can be given as follows:

$$\begin{aligned}
\xi &= (15+2\alpha)\sin^2\theta + (22\alpha-17)\cos\varphi\sin\theta\cos\theta \\
&\quad + \{(22\alpha-17)\sin\varphi\cos\varphi - (15+2\alpha)\sin^2\varphi\}\cos^2\theta\,, \\
\eta &= (25+12\alpha)\sin^2\theta + \{2\sin\varphi + (4\alpha-33)\cos\varphi\}\sin\theta\cos\theta \\
&\quad + \{(-27-12\alpha)\sin^2\varphi + (4\alpha-43)\sin\varphi\cos\varphi - 6\cos^2\varphi\}\cos^2\theta\,, \\
\zeta &= 1-(2\sin\varphi+5\cos\varphi)\sin\theta\cos\theta + 5(\sin\varphi\cos\varphi+\cos^2\varphi)\cos^2\theta\,.
\end{aligned}$$